

Supporting Information

Magnetically-Triggered Release of Entrapped Bioactive Proteins from Thermally Responsive Polymer-Coated Iron Oxide Nanoparticles for Stem Cell Proliferation

Matthew Walker, Iain Will, Andrew Pratt*, Victor Chechik*, Paul Genever*, Daniel Ungar*

* corresponding authors

Dr M Walker, Prof P Genever (paul.genever@york.ac.uk), Dr D Ungar (dani.ungar@york.ac.uk)
Department of Biology, University of York, York, YO10 5DD, UK

Dr I Will, Department of Electronic Engineering, University of York, York, YO10 5DD, UK

Dr A Pratt (andrew.pratt@york.ac.uk), Department of Physics, University of York, York, YO10 5DD, UK

Dr V Chechik (victor.chechik@york.ac.uk), Department of Chemistry, University of York, York, YO10 5DD, UK

Supplementary methods

All chemicals were purchased from Sigma-Aldrich unless otherwise stated.

Iron oxide nanoparticles (adapted from reference¹).

A 0.25 M solution of iron (II) chloride tetrahydrate in 1,2-propanediol (solution A) was heated to 180°C for 30 min. The same volume of half 5 M aqueous sodium hydroxide (NaOH) and half 1,2-propanediol (solution B) was heated to 100°C for 30 min and then injected into hot solution A. The combined mixture was refluxed for 1 h. The reaction was cooled to room temperature and quenched with MeOH of a volume equal to the total of A and B. Particles were collected and purified via centrifugation (4000 rpm, 10 min) followed by re-dispersion of pellets in MeOH (half of solution A volume) with sonication. The purification step was repeated 3 times. Purified nanoparticles were dried on a rotary evaporator. Yield: 4.7 g.

Acid-terminated PNIPAM (adapted from reference²).

NIPAM (1 g, 8.8 mmol), CuBr (13 mg, 0.09 mmol), CuBr₂ (2 mg, 0.009 mmol), and 2-methyl-2-bromopropionic acid (16.7 mg, 0.1 mmol) were dissolved in 9:1 (v/v) water:MeOH mixture under inert atmosphere and cooled to 0°C. A degassed solution of Me6TREN (Tokyo Chemical Industry, 40 µL, 0.15 mmol) in water (1 mL) was injected into the reaction mixture and left stirring for 16 h. After polymerisation, the reaction vessel was opened to air and heated to 50°C to precipitate out the polymer. The crude product was dissolved in THF (10 mL) and precipitated by pouring into ice-cold diethyl ether (40 mL). Yield: 930 mg (93%), M_n: 12.99 kDa, LCST: 32°C, ¹H NMR, δ, ppm (CDCl₃): 1.1 (br s, 6H, H¹), 1.5-2.5 (m, 3H, H²⁻³), 3.95 (br s, 1H, H⁴), 6.8 (br s, 1H, H⁵) (Figure S4a).

NDA-terminated PNIPAM (NDA-PNIPAM) (adapted from reference²).

PNIPAM (1 g, 0.1 mmol), 1-cyano-2-ethoxy-2-oxoethylidenaminoxy)dimethylamino-morpholino-carbenium hexafluorophosphate (COMU) (51 mg, 0.12 mmol) and *N,N*-diisopropylethylamine (DIPEA) (17 µL, 0.1 mmol) were dissolved in dry dimethylformamide (DMF) (20 mL) and stirring under nitrogen for 1 h at room temperature. 6-Nitrodopamine hydrogen sulfate (NDA)³ (89 mg, 0.3 mmol) and DIPEA (34 µL, 0.2 mmol) were dissolved in dry DMF (1 mL), injected into the PNIPAM reaction mixture and stirred under nitrogen at room temperature for 3 days. The reaction mixture was acidified with 2 M hydrochloric acid (HCl) before precipitating the polymer by pouring into ice-cold diethyl ether (80 mL). The precipitate was dissolved in a minimal amount of water (~10 mL), dialysed (M_w cut-off: 3.5 kDa) and dried on a rotary evaporator at 40°C. Yield: 750 mg, (75%), UV-vis NDA-functionality: 67% (Figure S5).

Polymer-coated nanoparticles (adapted from reference²).

NDA-PNIPAM (5 g) was added to a solution of iron oxide nanoparticles (1 g) in 1 mM aqueous sodium citrate (pH 7.4, 100 mL) in a 500 mL round-bottomed flask. The reaction mixture was sonicated for 5 h maintaining the temperature below 32°C and left at room temperature. The nanoparticles were collected by ultracentrifugation (50,000 rpm, 30 min) and redissolved in water. The centrifugation/dissolution step was repeated 3 times. Yield: 1.45 g, LCST: 32°C,

TGA: ~50% mass loss >400°C, grafting density: 0.66 chains/nm², XPS: 714.5 eV (Fe), 532.6 eV (O), 400.5 eV (N), 285.5 eV (C).

Nuclear magnetic resonance (NMR)

NMR was carried out in CDCl₃ or DMSO-*d*₆ on a JEOL ECS-400 spectrometer at 400 and 100 MHz for ¹H and ¹³C NMR, respectively. A 400 MHz field strength was used with 8 scans across a scan range of -2 to 12 ppm and scan acquisition time of 2 s for ¹H NMR. A 100 MHz field strength was used with 256 scans across a scan range of -60 to 240 ppm and scan acquisition time of 1 s for ¹³C NMR. Peak assignment was carried out using Structure-based Predictions in Nuclear Magnetic Resonance Spectroscopy (SPINUS) software⁴ using default parameters online (<http://joao.airesdesousa.com/spinus/>) to simulate spectra for comparison to experimental data.

Mass spectrometry

MALDI-TOF mass spectrometry was conducted on an Ultraflex II (Bruker) in positive linear ion mode with a SmartBeam laser at 60-80% power, and recorded over the 10,000-17,000 mass-to-charge ratio range using 2-(4-hydroxyphenylazo)benzoic acid (HABA) matrix.

Transmission electron microscopy

Nanoparticle suspension in dH₂O was sonicated for 15 min, one drop deposited onto 3 mm holey-carbon-coated copper grids, air-dried and imaged on a JEOL 2011 microscope operated at 200 kV. Images were extracted using Gatan Digital Micrograph software.

Vibrating sample magnetometry (VSM)

10 mg/mL nanoparticles in water were measured in an ADE Model 10 (Microsense) vibrating sample magnetometer equipped with a CF-1200 cryostat (Oxford Instruments) between 5 and 40°C. Magnetisation curves at each temperature were obtained by sweeping the field from -10 kOe to +10 kOe.

Magnetic susceptibility measurements and calculations

Magnetic susceptibility measurements were recorded on a Guoy balance (Sherwood Scientific, MK1 Magnetic Susceptibility Balance) using 10 mg/mL nanoparticles immobilised in a 1.5% agarose gel. Homogeneity was ensured by bath sonication throughout the sample preparation process.

Magnetic susceptibility was calculated using:

$$\text{a) } \chi_g = \frac{l}{m} c (R - R_o)$$
$$\text{b) } \chi_g (m^3 kg^{-1}) = (cgs) \cdot \frac{4\pi}{1000}$$

where χ_g is mass susceptibility, l is the sample length in the tube (cm), m is sample mass (g), c is the balance constant, R is the sample balance reading and R_o is the empty balance reading.

Equations a) and b) Magnetic susceptibility equations: a) Determination of mass

susceptibility (cgs) of samples from Guoy balance readings; **b)** Conversion from cgs into SI units (m^3kg^{-1}).

X-ray photoelectron spectroscopy (XPS)

XPS was conducted by drop casting nanoparticles (10 mg/mL) in aqueous solution onto silicon substrates. After solvent evaporation, dense layers of deposited nanoparticles were probed using a monochromated Al K α source (1486.6 eV, Omicron XM 1000) with a power of 220 W. Photoelectrons were detected using an Omicron EA 125 hemispherical energy analyser with a 2 mm entrance aperture and the sample normal oriented at 22.5° to both the X-ray source and entrance optics of the analyser.

Specific absorption rate (SAR) calculation

SAR was calculated using the following equation:

$$SAR = \frac{1}{mFe} C_{sol} m_{sol} \left(\frac{dT}{dt}\right)$$

where mFe is the mass of iron in the sample (g), C_{sol} is the specific heat capacity of the solvent ($C_{H_2O} = 4.184 \text{ J K}^{-1} \text{ g}^{-1}$), m_{sol} is the mass of solvent (g) and $dT(K) / dt$ (s) is the slope of temperature vs time.

Thermal gravimetric analysis

10 mg dry nanoparticle sample was pyrolysed at 25-600°C on a STA 625 (PL Thermal Sciences) under nitrogen at a ramp rate of 10°C/min.

Grafting density calculation

Polymer grafting density on the iron oxide nanoparticle surface was determined using an adapted calculation for TGA-derived grafting density (σ_{TGA}).² Briefly, the total number of polymer chains was calculated from the TGA-measured polymer mass loss between 200-600°C (50.3%), the mass of an individual particle derived from its radius (3.15 nm) and density (5.18 g/cm³ for magnetite), and the average polymer mass per chain (M_n of 12.99 kDa/6.02x10²³). The number of polymers per particle was then divided by the surface area of an individual particle calculated using the radius.

Magnetic heating

Samples cooled with a circulating fan were subjected to a 0.67 T, 108 kHz alternating magnetic field generated across a 10 mm gap in a proprietary instrument (Figure S7, S8). Water-cooled copper coils around a MnZn ferrite core generated the field.

Protein-loading of coated nanoparticles

1 mg PNIPAM-coated nanoparticles and 1 μg apotransferrin (Sigma) or 1 μg Wnt3a (R&D Systems) were dissolved in 100 μL buffer A (20 mM HEPES, 100 mM NaCl, pH 7.4), and incubated at 37°C for 1 h while shaking, followed by 1 h at room temperature under shaking. Excess protein was removed by magnetic separation between four 1 h washes with buffer A containing 10 mg/mL RNase B (for apotransferrin) or with DMEM containing 10% FBS (for

Wnt3a).

Protein release from coated SPIONs

Protein-loaded nanoparticles were incubated with 10 mg/mL RNase B in buffer A (for apotransferrin) or with 10% FBS containing DMEM (for Wnt3a) at the temperature and for the indicated times with or without magnetic treatment as described in the figure legends. Unless described differently in the figure legend, particles were magnetically separated at the time points before withdrawing 10 μ L for analysis (for apotransferrin) or allowing cellular assays to complete (for Wnt3a). For magnetic heating assays, temperature was measured using an infrared thermocouple probe.

Protein analysis by SDS-PAGE and western blotting

Samples were separated on 10% SDS-PAGE gels prior to coomassie staining or western blotting. Coomassie staining was carried out according to the method of Fairbanks,⁵ modified by boiling the gel in each of the staining/destaining buffers.

For western blotting the proteins were transferred onto PVDF membranes by semi-dry transfer and probed with anti-apotransferrin (1:1000, Dako) in the presence of 5% milk in PBS-Tween20 buffer overnight at 4°C. Following secondary antibody binding, blots were imaged on a GeneGenius Chemi-imager (Syngene) after application of Immobilon HRP substrate (Millipore). Quantification was carried out using ImageJ software.

Cell culture

Y201 hTert MSCs⁶ and the MSC Wnt reporter line⁷ were cultured in Dulbecco's Modified Eagle Medium (Invitrogen) supplemented with 10% fetal bovine serum (Invitrogen) and 1% penicillin/streptomycin (Invitrogen) as published. Custom-made cell growth tubes for magnetic heating were designed in-house (35 mm x 20 mm x 8 mm, Figure S10), the base and lids of the tubes consist of polyether ether ketone (PEEK), and tube bases were secured to glass sides (flame polished) with a silicon O-ring.

Wnt reporter assays

Wnt reporter MSCs⁷ were seeded at 17,500 cells/cm² and grown overnight before incubation with Wnt3a overnight at the indicated temperature. If necessary, SPIONs were removed by magnetic separation. Cells were washed three times with 200 μ L PBS, then detached with trypsin and analysed by flow cytometry (CyAn ADP, Beckman Coulter). Results were gated for eGFP-positive (488 nm) live cells using the Summit software (v4.3.04, using default parameters).

MSC proliferation and viability

Y201 MSCs were seeded into custom-made tubes at 3500 cells/cm². The following day SPIONs (or Wnt3a for calibration curve) were added, subjected to magnetic heating as indicated, then nanoparticles were magnetically removed, and the cells incubated at 37°C for 5 days to assay proliferation or 7 days to assess cell viability. Cells were then washed once with carbonate buffer (0.133 M Na₂CO₃, 0.066 M NaHCO₃) before adding 150 μ L 0.1% Triton-X100 in carbonate buffer. Cells were then freeze/thawed three times while applying manual agitation,

and 50 μ L lysate transferred into a black opaque 96 well plate (Greiner) and 50 μ L picogreen reagent (Quant-iT PicoGreen dsDNA Reagent, Invitrogen, 50x diluted in 100 mM Tris, 1 mM EDTA, pH 7.5) was added. After rocking for 5 min at room temperature fluorescence was determined on a Clariostar plate reader (BMG Labtech) using 485 nm excitation and 538 nm emission wavelength.

Statistics

Details of the applied statistical tests and the number or replicate measurements are included in the relevant figure legends.

Supplementary data

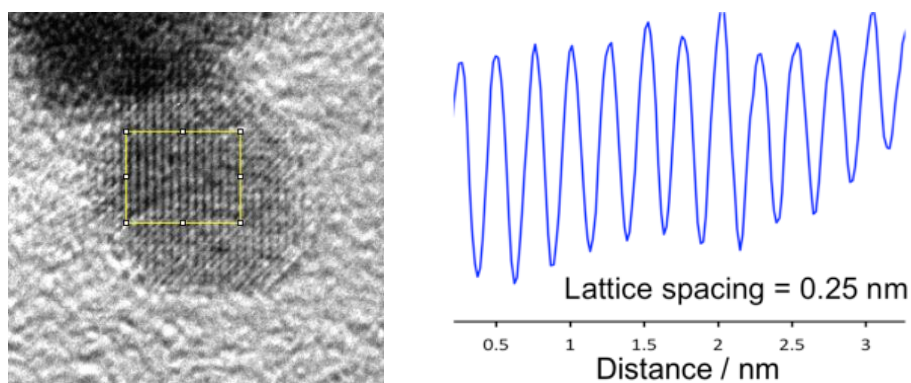


Figure S1. Measurement of SPION lattice spacing

(Left) The SPION image from Figure 1c was rotated to allow for the use of an averaged line scan over the area highlighted in the yellow box in Image J. (Right) The plot shows the obtained average line scan, where the total distance over 12 planes was measured as 3.02 nm. Fast Fourier transform analysis of the same nanoparticle image using ImageJ results in the same lattice spacing of 0.25 nm.

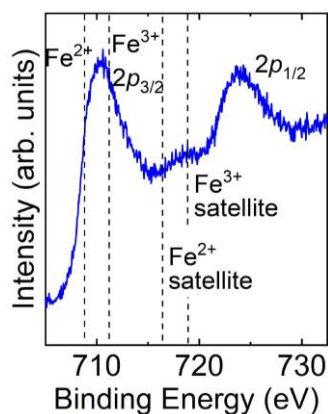


Figure S2. XPS spectrum of the Fe 2p states in the SPION sample.

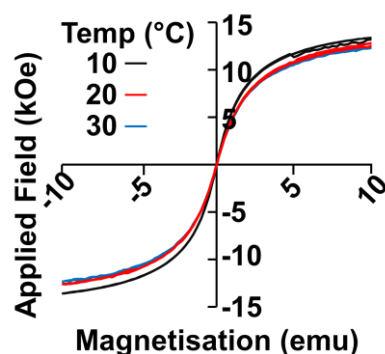


Figure S3. Vibrating sample magnetometry (VSM) analysis of SPIONs.

10 mg/mL aqueous SPION samples, recorded across an applied field of -10 to 10 kOe with forward and reverse field sweeps taken at the indicated temperatures.

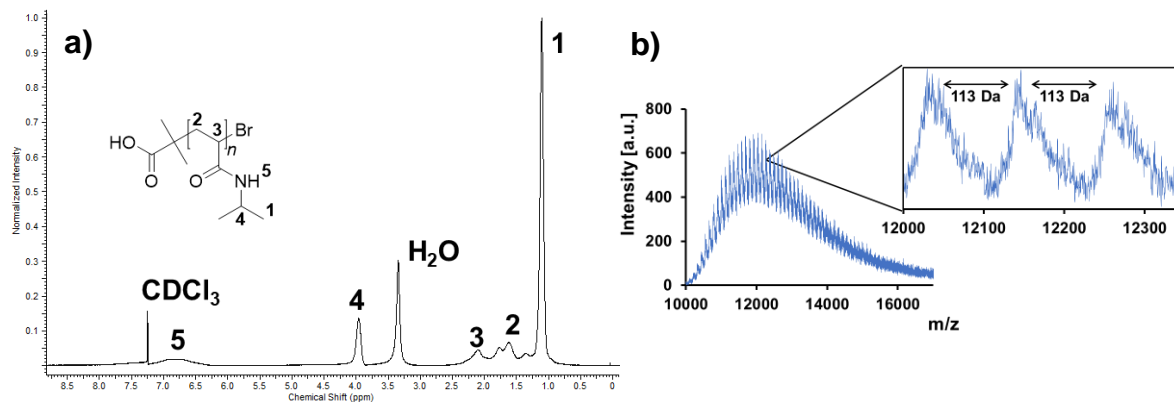


Figure S4. Characterization of PNIPAM

a) ^1H NMR spectrum of acid-terminated PNIPAM at 10 mg/mL dissolved in CDCl_3 .

Characteristic PNIPAM peaks detected at: ^1H NMR, δ , ppm (CDCl_3): 1.1 (br s, 6H, H^1), 1.5-2.5 (m, 3H, $\text{H}^{2,3}$), 3.95 (br s, 1H, H^4), 6.8 (br s, 1H, H^5).

b) MALDI mass spectrum of acid-terminated PNIPAM spotted from a 1 mg/mL solution, acquired between mass range 10-17 kDa. Inset (top right) shows spacings between polymer peaks of 113 Da ($M_n = 12.99$ kDa).

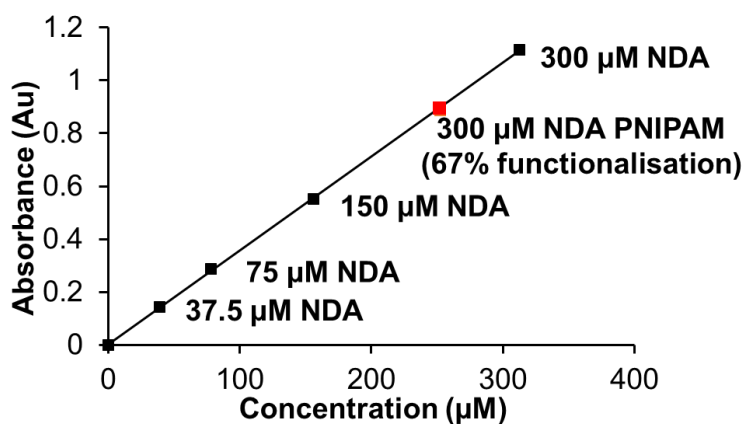


Figure S5. Functionalization of PNIPAM with NDA

Calibration curve of NDA standards from 37.5 – 300 μM to generate a linear regression where the $R^2 = 0.99$, alongside 300 μM NDA-PNIPAM. NDA-PNIPAM concentration was determined using M_n of acid-terminated PNIPAM plus the mass of a terminating molecule of NDA.

Absorbance readings collected at λ_{max} (350 nm) were used for the formula: $(\text{absorbance} - 0.0027)/0.0036$ to determine NDA concentration in PNIPAM. Samples were analysed in a 1 mM sodium citrate buffer, pH 5.5.

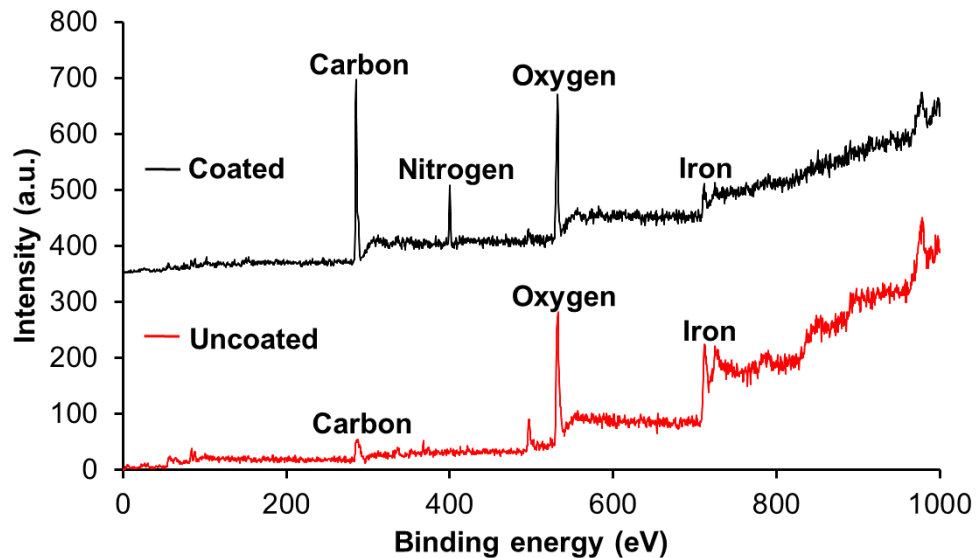
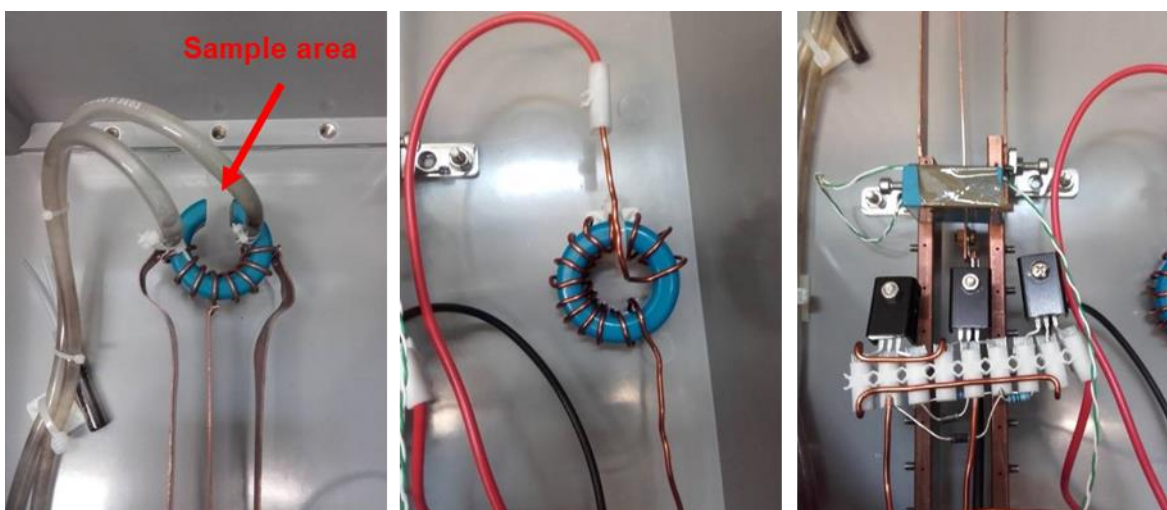


Figure S6. XPS of uncoated and PNIPAM-coated iron oxide nanoparticles.

Using 10 mg/mL samples of uncoated and PNIPAM-coated iron oxide nanoparticles, peaks were detected by X-ray photoelectron spectroscopy (XPS) across a range of 0 – 1000 eV binding energy. Elemental peaks were detected at: 714.5 eV, iron (Fe), 532.6 eV, oxygen (O), 285.5 eV, carbon (C) for both uncoated and PNIPAM-coated particles, and also at 400.5 eV, nitrogen (N) in coated particles.

a)



b)

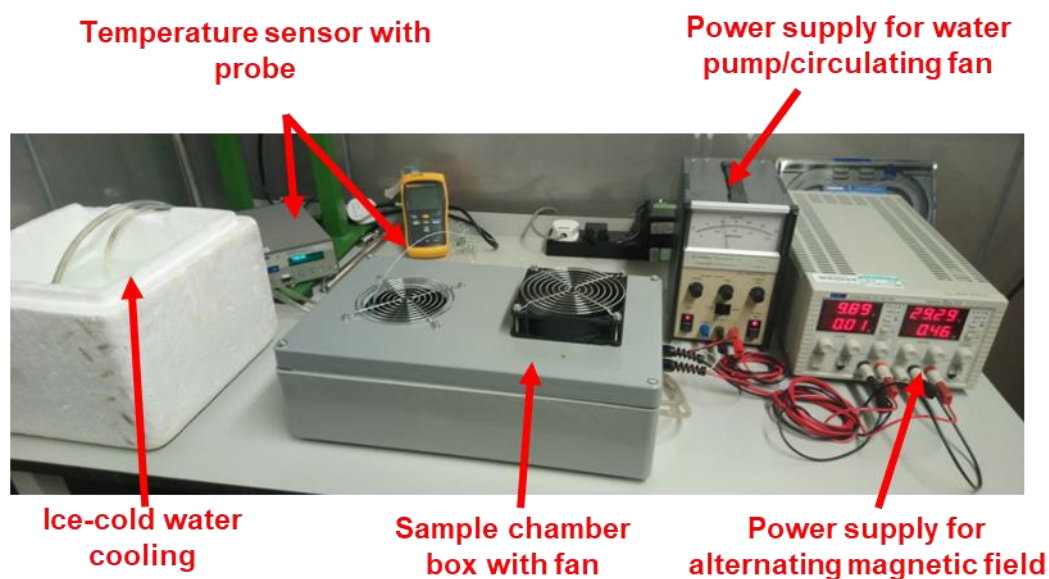


Figure S7. Magnetic heating setup.

a) Internal components of sealed box, showing the sample area for magnetic heating (red). Also shown are: (left image) the ferrite core, induction coil and electrical connections with centre tap power conductor in the centre; (central image) the choke; and (right image) the transistor circuit.

b) The entire experimental setup, showing from left to right: ice-water box for coil cooling, infrared thermocouple with probe, sample chamber box with circulating fan, power box for circulating fan/ice-water coil cooling and power box for the alternating magnetic field.

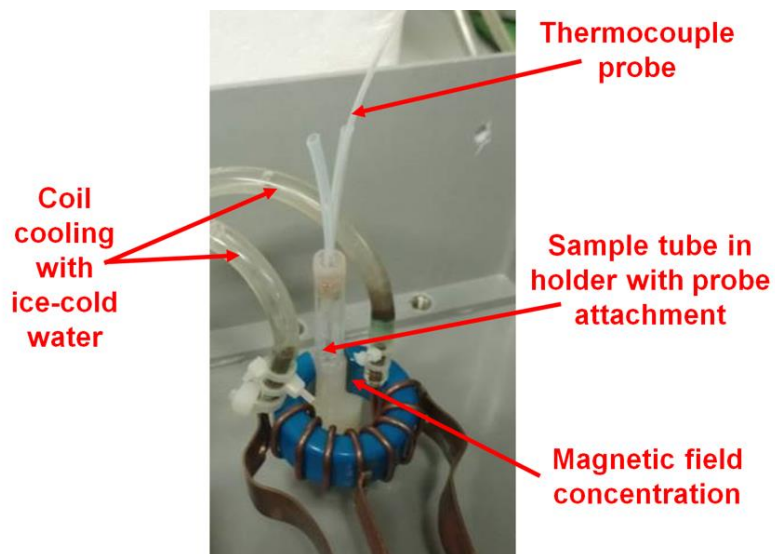


Figure S8. Sample setup for magnetic heating experiments.

The sample-specific area for the magnetic heating assays contained within the sealed box. Samples were positioned in an area that the alternating magnetic field was focused on. Annotations highlight specific components in this area, including: the thermocouple probe, which was inserted through an adapted inlet for temperature readings; and tubing, which was used to pump ice-cold water through coils surrounding the magnet.

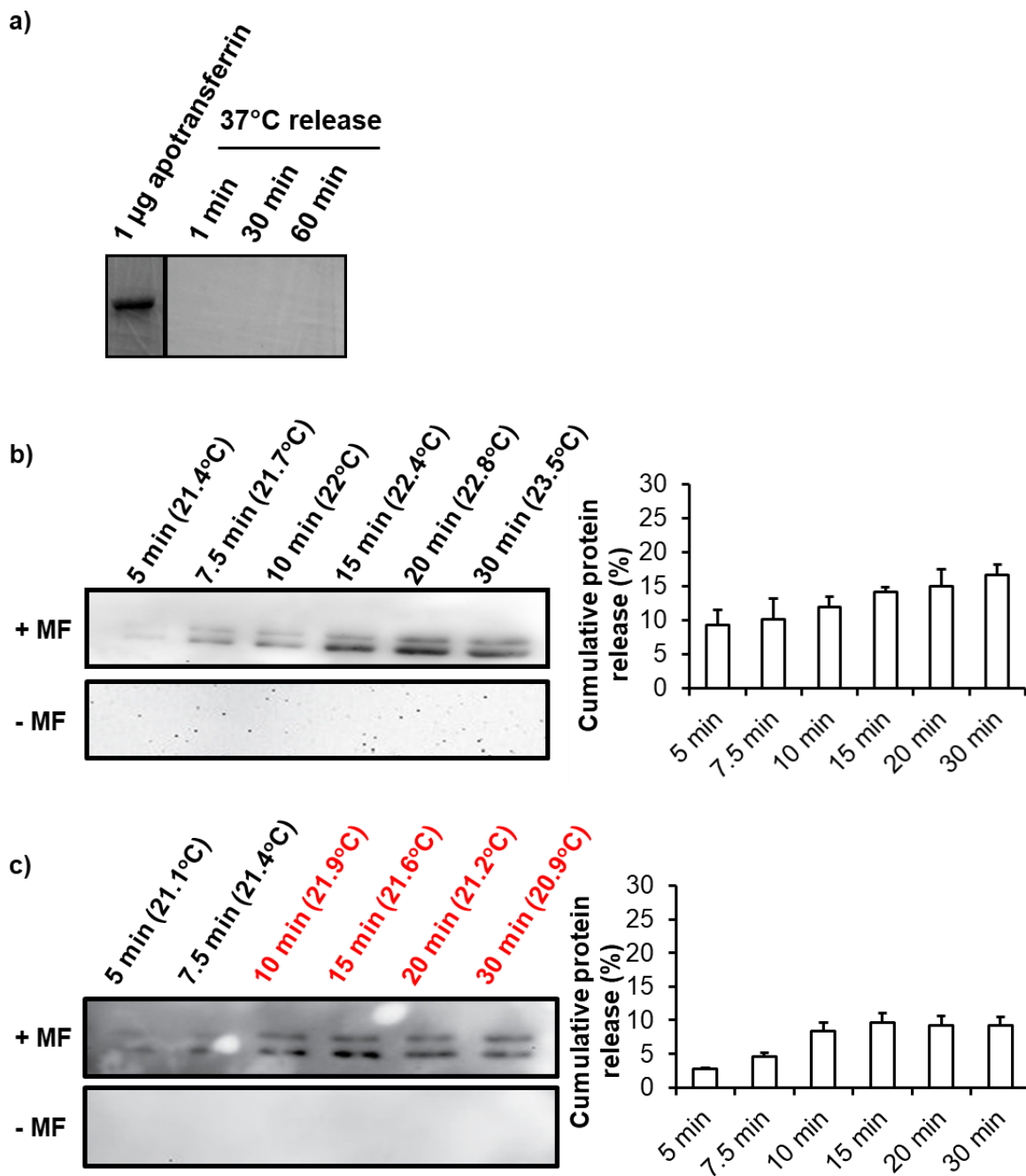


Figure S9. Release of the model protein apotransferrin from polymer coated SPIONs.

a) 1.2 µg apotransferrin loaded into 1 mg coated SPIONs was incubated at 37°C in physiological buffer without the addition of any competing proteins, and at the indicated times the particles magnetically removed and the solution sampled. Samples were run on SDS-PAGE and coomassie stained. The apotransferrin in the first lane was run on the same gel, but not next to the release samples, hence the lane was moved, and this is indicated with a black divider line. The rest of the lanes contained wash samples, used to wash away excess apotransferrin following the loading step. **b)** Western blot analysis of the apotransferrin collected

from the supernatant, following incubation of 1 mg apotransferrin loaded PNIPAM-coated nanoparticles in the presence of 10 mg/mL RNase B at pH 7.5 with or without magnetic heating (+/-MF). SPIONs were briefly collected on one side of the tube with a permanent magnet when the solution was sampled at the indicated time points. Temperatures measured during magnetic heating are shown in brackets above each time point. The sample without magnetic heating was maintained at 21°C. Densitometry of the apotransferrin immunoblot signal was used to quantify the release of apotransferrin. Error bars denote standard deviation, n=3. **c)** As in 'b' except that the magnetic field was turned off at the 10 min time point for the remainder of the experiment.

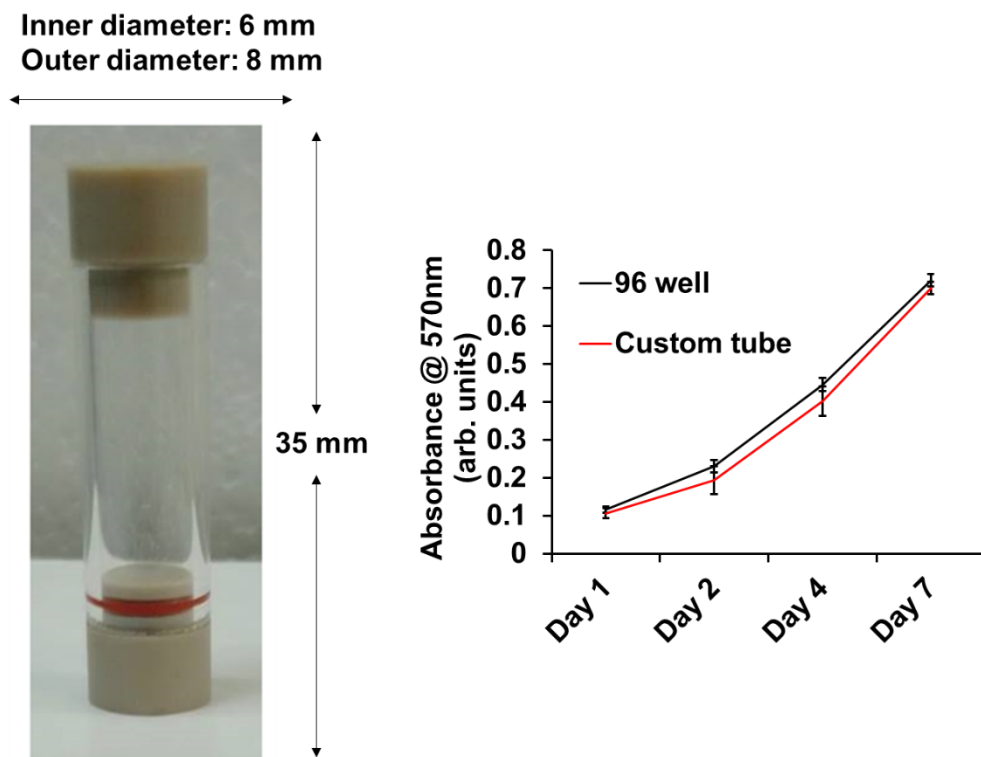


Figure S10. The characterisation of custom-made vessels for cell magnetic heating experiments.

Image of a custom-made vessel and its dimensions; and results of the MTT proliferation assay⁸ on Y201 MSCs seeded in custom-made tubes or in 96 well plates at 3500 cells/cm² and cultured over 7 days. n=3, error bars denote standard deviation.

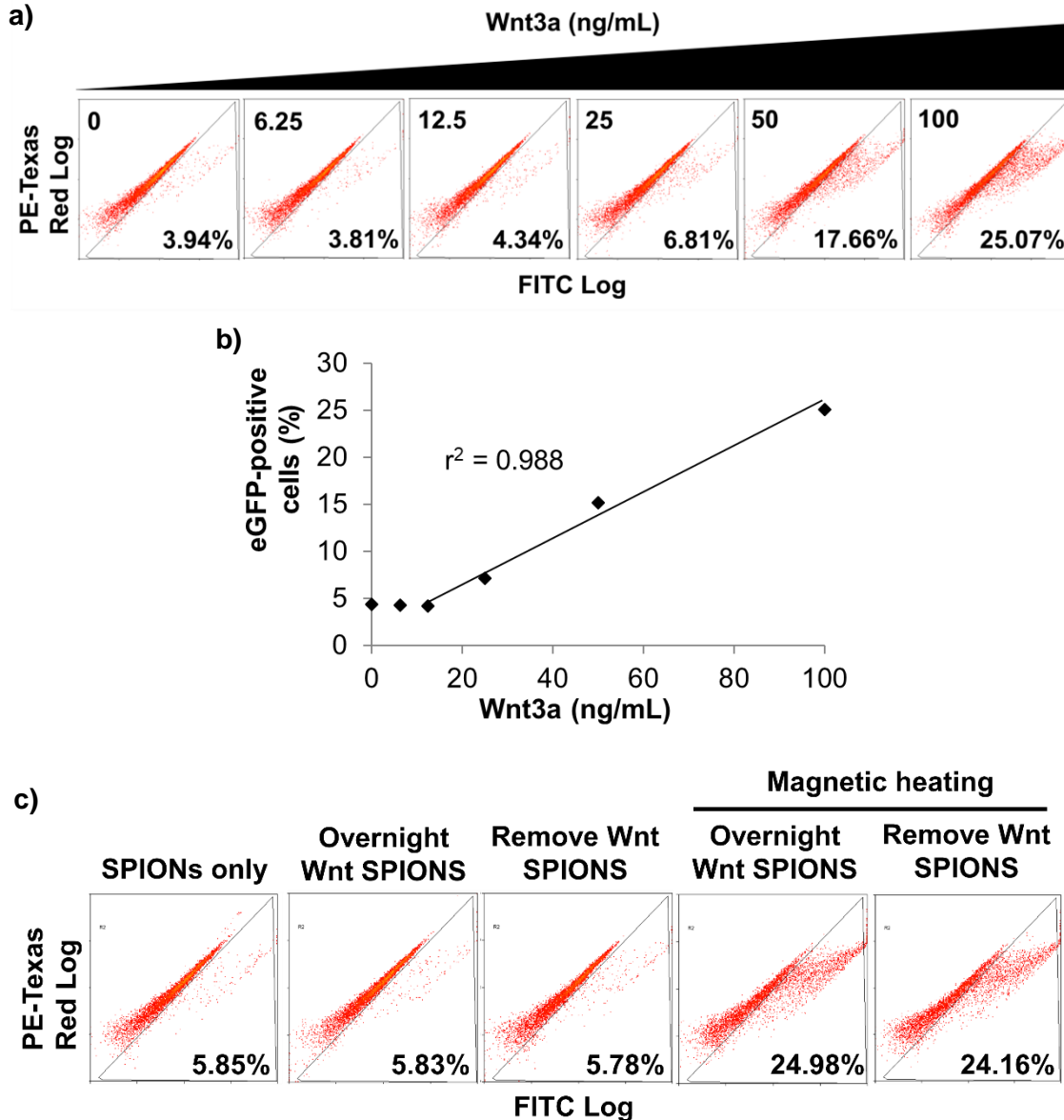


Figure S11. The Wnt-reporter MSC line shows a linear dose-response both at 30°C and 37°C.

a) Representative flow cytometry scatter plots showing eGFP expression levels of Y201 Wnt-reporter cells, following overnight incubation at 30°C with the indicated concentrations of Wnt3a. The percentage of eGFP positive cells is indicated in the bottom right corner of each plot. The line in each plot indicates the threshold, above which cells were classed as eGFP positive. Emission at the wavelength of Texas-red was used to control for non-specific staining. **b)** Calibration curve derived from the scatter plots. Calibration curves were determined each time a Wnt-reporter experiment was performed. Each calibration curve was derived from data points determined using biological duplicates. **c)** Representative scatter plots of the Wnt-reporter experiments for which the quantification is shown in Figure 3b.

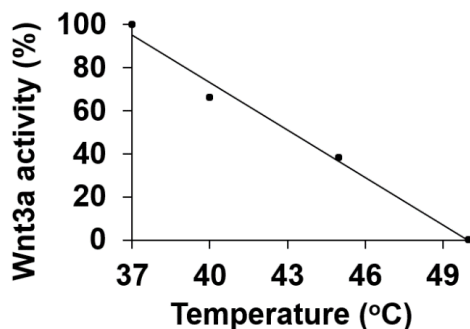


Figure S12. Temperature dependence of Wnt3a activity above 37°C

Wnt3a was incubated for 10 min at the indicated temperature before incubating it with Wnt-reporter cells overnight. Wnt3a activity was then calculated using the eGFP-positive Wnt reporter MSC response relative to a control sample kept at 37°C. A line of best fit is shown.

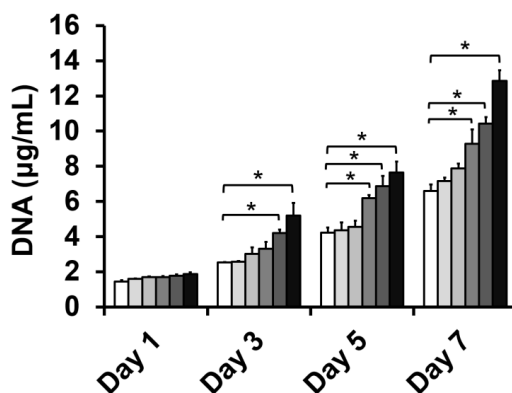


Figure S13. Dose response relationship between Wnt3a concentration and MSC proliferation.

1000 Y201 MSCs per well were cultured in the presence of the indicated Wnt3a concentration in a 96 well plate. The DNA quantities were then determined on the indicated days using picogreen staining and a standard curve derived from salmon sperm DNA. Error bars represent standard deviation, $n=3$, * indicates $p<0.05$ using Kruskal-Wallis One Way ANOVA on Ranks, followed by Dunn's post hoc test.

Supplementary References

- (1) Carroll, K. J.; Shultz, M. D.; Fatouros, P. P.; Carpenter, E. E. High magnetization aqueous ferrofluid: A simple one-pot synthesis. *J Appl Phys* 2010, 107 (9), 09B304.
- (2) Kurzahls, S.; Zirbs, R.; Reimhult, E. Synthesis and Magneto-Thermal Actuation of Iron Oxide Core-PNIPAM Shell Nanoparticles. *ACS Appl Mater Inter* 2015, 7 (34), 19342-19352.
- (3) Napolitano, A.; Dischia, M.; Costantini, C.; Prota, G. A New Oxidation Pathway of the Neurotoxin 6-Aminodopamine - Isolation and Characterization of a Dimer with a Tetrahydro[3,4a]Iminoethanophenoxazine Ring-System. *Tetrahedron* 1992, 48 (39), 8515-8522.

- (4) Aires-de-Sousa, J.; Hemmer, M. C.; Gasteiger, J. Prediction of H-1 NMR chemical shifts using neural networks. *Anal Chem* 2002, *74* (1), 80-90.
- (5) Fairbanks, G.; Steck, T. L.; Wallach, D. F. H. Electrophoretic Analysis of Major Polypeptides of Human Erythrocyte Membrane. *Biochemistry* 1971, *10* (13), 2606-2617.
- (6) James, S.; Fox, J.; Afsari, F.; Lee, J.; Clough, S.; Knight, C.; Ashmore, J.; Ashton, P.; Preham, O.; Hoogduijn, M.; Ponzoni Rde, A.; Hancock, Y.; Coles, M.; Genever, P. Multiparameter Analysis of Human Bone Marrow Stromal Cells Identifies Distinct Immunomodulatory and Differentiation-Competent Subtypes. *Stem Cell Rep* 2015, *4* (6), 1004-1015, DOI: 10.1016/j.stemcr.2015.05.005.
- (7) Saleh, F.; Carstairs, A.; Etheridge, S. L.; Genever, P. Real-Time Analysis of Endogenous Wnt Signalling in 3D Mesenchymal Stromal Cells. *Stem Cells Int* 2016, *2016*, 7132529.
- (8) Wilson, K. M.; Jagger, A. M.; Walker, M.; Seinkmane, E.; Fox, J. M.; Kroger, R.; Genever, P.; Ungar, D. Glycans modify mesenchymal stem cell differentiation to impact on the function of resulting osteoblasts. *J Cell Sci* 2018, *131* (4), jcs209452, DOI: 10.1242/jcs.209452.